

A New Generation of ICRP Reference Pediatric Computational Phantoms

Chansoo Choi^a, Bangho Shin^a, Haegin Han^a, Yeon Soo Yeom^b, Sungho Moon^a, Sangseok Ha^a, Chan Hyeong Kim^{a*}

^a Department of Nuclear Engineering, Hanyang University, 222 Wangsimni-ro, Seongdong-gu, Seoul 04763, Korea

^b National Cancer Institute, National Institute of Health, 9609 Medical Center Drive, Bethesda, MD 20850, USA

* Corresponding author: chkim@hanyang.ac.kr

1. Introduction

Since the 2007 Recommendation was issued [1], the International Commission on Radiological Protection (ICRP) has released a set of the adult and pediatric reference computational phantoms in voxel format [2, 3], called ‘Voxel-type Reference Computational Phantoms (VRCPs)’, to produce reference dose values for various exposure scenarios of interest in the ICRP. While they provide relatively realistic representations of the human anatomy compared to older stylized phantoms, the VRCPs do not accurately represent small or complex organs and tissues below their voxel resolutions, which leads to unreliable dose calculations particularly for weakly-penetrating radiations [4]. Moreover, due to the inherent nature of voxel geometry, it is difficult to deform the VRCPs into phantoms in different postures and body sizes, which is needed for individual dose reconstructions in medical or accidental exposures.

In 2016, to address the limitations of the VRCPs, the ICRP established Task Group 103 (TG 103) within ICRP Committee 2, the ultimate mission of which is to develop mesh counterparts of the VRCPs, named ‘Mesh-type Reference Computational Phantoms (MRCPs)’. Of note is that the mesh geometry is currently recognized as the most advanced format for the phantom development [5]. Recently, the TG 103 successfully developed the MRCPs for the adult male and female, by converting the adult VRCPs into a high-quality/fidelity mesh format [6]. The adult MRCPs will be released in upcoming ICRP Publication (i.e., ICRP *Publication 145*) later this year.

Following the release of the adult MRCPs, in the present study we developed the pediatric MRCPs by converting the pediatric VRCPs into a mesh format, basically following the approach used for the adult MRCPs. For the organs and tissues which cannot directly converted from the pediatric VRCPs, modification or modelling approaches were used. The micron-thick target and source regions prescribed by the ICRP were also defined in the pediatric MRCPs. After the phantom construction, the pediatric MRCPs were implemented into the Geant4 Monte Carlo code [7] to calculate organ absorbed and effective doses for external exposures to photons and electrons, and the results were compared with those of the pediatric VRCPs to investigate the dosimetric impact of the new phantoms.

2. Materials and Methods

2.1 Overview of pediatric VRCPs

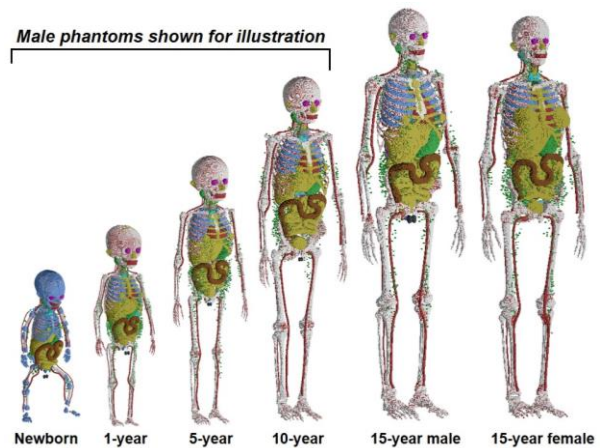


Figure 1. A set of pediatric VRCPs. The figure shows only male phantoms for 10 years and younger.

Figure 1 shows the current reference phantoms, i.e., pediatric VRCPs. The pediatric VRCPs consists of ten phantoms representing the reference male and female at five different ages (i.e., newborn, 1 year, 5 years, 10 years and 15 years). The pediatric VRCPs are composed of ~50 million voxels with resolutions ranging from hundreds of micrometers to several millimeters depending on age. The phantoms contain 48 organ/tissue groups basically required for effective dose calculations. The standing height and total body mass and organ tissue masses of the pediatric VRCPs were all matched to the reference values given in ICRP *Publication 89* [8]. It should be noted that the pediatric VRCPs were constructed from the UF/NCI pediatric phantom series [9] by voxelization process with several modifications and additions of some organs and tissues.

2.2 Construction of pediatric MRCPs

Most of the simple organs and tissues of the pediatric MRCPs were produced using both the pediatric VRCPs and the UF/NCI pediatric phantoms. Note that most of the organs and tissues of the UF/NCI phantoms are in Non-Uniform Rational B-Spline (NURBS) format which can be more easily converted into mesh models than voxel structures. First, the organs and tissues of the UF/NCI phantoms were converted into primitive mesh models through surface rendering and refinement procedure using the 3D rendering programs, following the approach used for the adult MRCPs [6]. The primitive mesh models were then adjusted to those of the

pediatric VRCPs to preserve the topology of the pediatric VRCPs. Then, several organs and tissues (e.g., cranium, spine and hand/foot bones, colon, thyroid, extra-thoracic (ET) regions, eyes, lymphatic nodes, teeth, blood in large vessels, muscle, and exterior body contour), which are imprecisely represented or anatomically incorrect in the pediatric VRCPs, were remodeled or modified in the pediatric MRCPs, referring to scientific literatures under the guidance of the anatomists.

The organs and tissues of the pediatric MRCPs were adjusted to reference masses inclusive of blood content. The pediatric VRCPs were matched to the reference organ/tissue masses listed in Table 2.8 of ICRP *Publication 89* [8], which represent the parenchyma masses of the organs and tissues, i.e., not including intra-organ blood masses. In a living person, however, a large portion of the blood is included in the small vessels and capillaries in the organs and tissues, which should be considered for the phantom construction. In the present study, therefore, the organ/tissue masses and densities were recalculated by using the regional blood volume fractions for each age [10]. The organ/tissue volumes were then globally enlarged, thereby matching the blood-inclusive reference masses and densities.

Finally, the micron-scale radiosensitive and source layers were included in the respiratory and alimentary tract organs, skin, and urinary bladder. The target and source layers of the respiratory and alimentary tract organs were defined following the age-dependent morphometric data given in ICRP *Publication 66* and *100* [11, 12], respectively. The target layers of the skin and urinary bladder were defined following the age-dependent depth and thickness data recently determined by ICRP Committee 2.

2.3 Monte Carlo dose calculations

The pediatric MRCPs were used to calculate the organ absorbed and effective dose for external exposures to photons in antero-posterior (AP), postero-anterior (PA), left-lateral (LLAT), right-lateral (RLAT), rotational (ROT), and isotropic (ISO) directions and electrons in AP, PA, and ISO directions. The calculated dose values were then compared with values calculated with the pediatric VRCPs. For the dose calculations, the pediatric MRCPs were implemented in the Geant4 code (version 10.06) using the *G4Tet* class. Primary particle energies ranging from 10 keV to 10 GeV were considered and the physics library of *G4EMLiverMorePhysics* was used. The statistical errors for the organ absorbed and effective doses were less than 5% and 0.5%, respectively.

3. Results and Discussion

3.1 Pediatric MRCPs

Figure 2 shows the pediatric MRCPs developed in the present study. As with the pediatric VRCPs, the pediatric MRCPs consist of ten phantoms representing male and

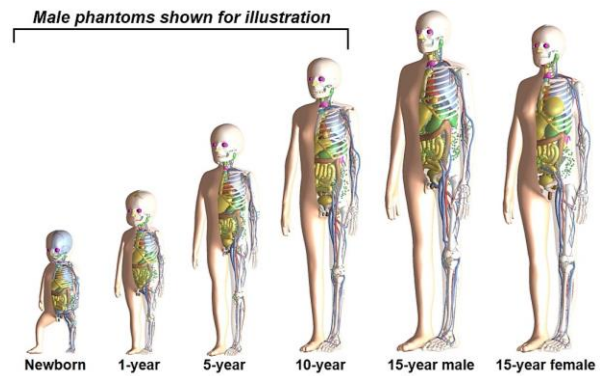


Figure 2. A set of pediatric MRCPs developed in the present study. The figure shows only male phantoms for 10 years and younger.

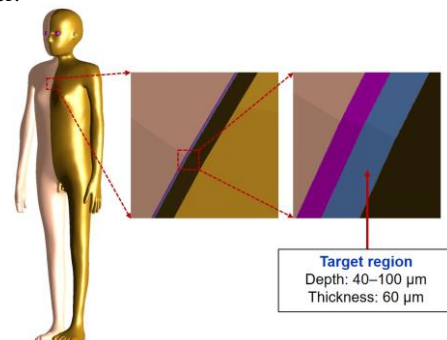


Figure 3. Target region defined in the skin of the 10-year male MRCP.

female at five different ages and the standing height and total body mass were precisely matched to reference data of ICRP *Publication 89* [8]. The MRCPs are in tetrahedral-mesh format composed of approximately six to seven million tetrahedra. The pediatric MRCPs equally contain 48 organ/tissue groups but include the tens-of-micron-scale target and source layers in the respiratory and alimentary tract organs, skin, and urinary bladder (see Figure 3). The masses of the organs and tissues are in accordance with the reference values inclusive of blood content within 0.1% of deviation.

3.2 Comparison of organ/tissue absorbed and effective dose

The comparison analysis showed that for photons, except for very low energies, the organ absorbed doses for most organs and tissues and effective doses of the pediatric MRCPs were generally in a good agreement with those of pediatric VRCPs. For electrons, however, the dose values of the pediatric MRCPs were significantly different from those of the pediatric VRCPs, particularly for the organ absorbed doses of the superficial organs and tissues (e.g., skin) and the skeletal tissues (e.g., red bone marrow (RBM)), due to the fact that the representation of these organs and tissues was significantly improved in the pediatric MRCPs. Figure 4, as an example, shows the ratio of RBM absorbed doses of the pediatric MRCPs with respect to those of the

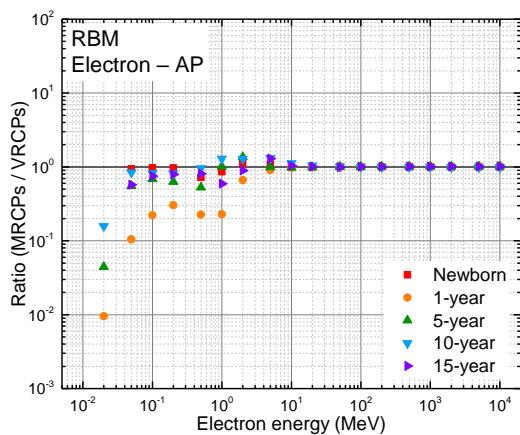


Figure 4. Ratio of RBM absorbed doses of pediatric MRCPs with respect to those of pediatric VRCPs for electrons in AP direction.

pediatric VRCPs for electrons in AP direction. It can be seen that for low energy regions (< 10 MeV), the values of the pediatric MRCPs are generally smaller than those of the pediatric VRCPs by up to a factor of ~ 100 ; this is because the spongiosa region where the RBM presents is completely covered by the cortical bone in the pediatric MRCPs, whereas that of pediatric VRCPs is exposed to the outside of cortical bone due to the limited voxel resolution.

4. Conclusion

In the present study, a set of the pediatric MRCPs were developed by converting the pediatric VRCPs to a high-quality/fidelity mesh format to address the limitations of the VRCPs. In addition, organ absorbed and effective doses were calculated by using the pediatric MRCPs for photons and electrons and compared with those of the pediatric VRCPs. The comparison showed that in general, the pediatric MRCPs provide very similar dose values for photons but provide significantly different dose values for electrons. Considering the geometric and anatomical improvements of the pediatric MRCPs, the new phantoms are expected to provide more accurate and reliable dose values for children and adolescents.

REFERENCES

- [1] ICRP, The 2007 recommendations of the International Commission on Radiological Protection, ICRP Publication 103, Ann. ICRP 32 (2-4), 2007.
- [2] ICRP, Adult reference computational phantoms, ICRP Publication 110, Ann. ICRP 39 (2), 2009.
- [3] ICRP, Paediatric reference computational phantoms, ICRP Publication 143, 2020 (in press).
- [4] ICRP, Conversion coefficients for radiological protection quantities for external radiation exposures, ICRP Publication 116, Ann. ICRP 40 (2-5), 2010.
- [5] W. Kainz, E. Neufeld, W.E. Bolch, et al., Advances in computational human phantoms and their applications in biomedical engineering, a topical review IEEE Trans. Radiat. Plasma Med. Sci., Vol. 3, pp. 1-23, 2019.

[6] C.H. Kim, Y.S. Yeom, T.T. Nguyen, et al., New mesh-type phantoms and their dosimetric applications, including emergencies, Ann. ICRP 47, pp. 45-62, 2018.

[7] J. Allison, K. Amako, J. Apostolakis, et al., Recent developments in Geant4, Nucl. Instrum. Methods Phys. Res. Sect. A., Vol. 835, pp. 186-225, 2016.

[8] ICRP, Basic anatomical and physiological data for use in radiological protection: reference values, ICRP Publication 89, Ann. ICRP 32 (3-4), 2002.

[9] C. Lee, D. Lodwick, J. Hurtado, et al., The UF family of reference hybrid phantoms for computational radiation dosimetry, Phys. Med. Biol., Vol. 55, pp. 339-363, 2010.

[10] M.B. Wayson, R.W. Leggetti, D.W. Jokisch, et al., Suggested reference values for regional blood volumes in children and adolescents, Phys. Med. Biol., Vol. 63, 155022, 2018.

[11] ICRP, Human respiratory tract model for radiation protection, ICRP Publication 66, Ann. ICRP 24 (1-3), 1994.

[12] ICRP, Human alimentary tract model for radiation protection, ICRP Publication 100, Ann. ICRP 36 (1-2), 2006.